Fluctuations and destabilization of single phospholipid bilayers

T. Charitat[a] and S. Lecuyer
Institut Charles Sadron, Université Louis Pasteur, CNRS, 23 Rue du Loess, BP 84047, 67034 Strasbourg Cedex 2, France

G. Fragneto
Institut Laue-Langevin, F-38042 Grenoble, France

(Received 12 March 2008; accepted 5 May 2008; published 23 June 2008)

Supported phospholipid bilayers are interesting model systems for biologists and present fascinating physical properties. The authors present an extensive experimental study of the dynamic properties of supported bilayers. The structure and the equilibrium properties of single and double supported bilayers were investigated with neutron reflectivity. The submicronic fluctuation spectrum of a nearly free "floating" bilayer was determined using off-specular x-ray scattering: the surface tension of the bilayer, its bending modulus, and the intermembrane potential could be determined. Using fluorescence microscopy, the authors showed that this well-controlled single bilayer can form vesicles. Destabilization occurred either at the main gel-fluid transition of the lipids and could be interpreted in terms of a decrease in the bending rigidity or under an ac low-frequency electric field applied in the fluid phase. In the latter case, the authors also studied the effect of the electric field at the molecular length scale by neutron reflectivity. In both cases, destabilization leads to the formation of relatively monodisperse vesicles. This could give further understanding on the vesicle formation mechanism and on the parameters that determine the vesicle size. © *2008 American Vacuum Society.* [DOI: 10.1116/1.2936938]

I. INTRODUCTION

A. Amphiphilic molecules and self-assembled systems

Amphiphilic molecules possess both hydrophilic and hydrophobic properties. A large variety of synthetic and natural molecules, such as copolymers, proteins, fatty acids, phospholipids, and saponins, are amphiphilic. The hydrophobic part is generally formed by one or two aliphatic chains. The hydrophilic part can be neutral (e.g., a polar group in alcohols) or charged: negatively (as in sodium dodecyl sulfate), positively (as in cetyltrimethylammonium bromide), or both (as in zwitterionic phosphatidylcholine lipids).

Due to these antagonistic affinities, amphiphilic molecules present complex behaviors. Their tensioactive properties result from the ability to stabilize interfaces. In solution, they can also self-assemble into complex, thermodynamically stable, or metastable structures.

These complex structures present a first level of self-organization: spherical or cylindrical micelles, bilayers, etc.[1–3] A second level of organization is also possible, such as hexagonal, lamellar, sponge, or cubic phases, as well as vesicles of various morphologies and topologies. Simple geometrical considerations can give important qualitative information on the behavior of a specific type of amphiphilic molecule; one can define the reduced specific volume $\mathcal{V}$ from the molecular volume v, the mean area per hydrophilic head a_0, and the chain length ℓ (see Fig. 1):

$$\mathcal{V} = \frac{v}{a_0 \ell}. \tag{1}$$

When $\mathcal{V} < 1/3$, the molecules tend to form spherical micelles. If $1/3 < \mathcal{V} < 1/2$, they form cylindrical micelles, whereas lamellar phases are usually observed for $\mathcal{V} > 1/2$.

In the case of phospholipids, which have two short hydrophobic chains, the specific reduced volume is of the order of 1 (area/lipid $a_0 \sim 50$ Å^2, chain length $\ell \sim 20$–30 nm, lipid molecular volume $v \sim 1000$ Å^3). Phospholipids thus self-assemble into bilayers, which can, in turn, form various structures: periodic lamellar phases, L_α, multiconnected lamellar phases (cubic or sponge phase, L_3), or vesicles, L_4. Single phospholipid bilayers can also be deposited on a hydrophilic flat substrate using Langmuir-Blodgett transfer technique[4,5] or fusion of vesicles.[6,7]

B. Lipid membrane: A model system for physicists and biophysicists

Phospholipids self-assemble in aqueous solutions to form bilayers of a few nanometers in thickness, leading to many different lamellar geometries: spherical or cylindrical vesicles and liposomes made from one or a few bilayers, multilamellar ordered or disordered systems, surface supported bilayers, and black lipid membranes (see Fig. 2).[4,8–10] For the physicist, phospholipid bilayers are two-dimensional model systems exhibiting a wide range of fascinating properties.[8,9] Seminal work by Canham[11] and Helfrich,[12] who first recognized the importance of the membrane bending elasticity, paved the way for extensive studies that contributed to the writing of one of the finest chapters in statistical physics of soft condensed matter. Lipid bilayers can be

[a]Electronic mail: charitat@ics.u-strasbg.fr

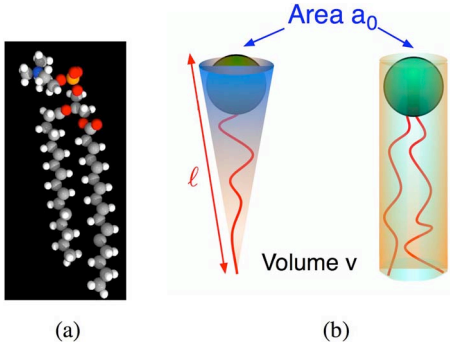

FIG. 1. Example of amphiphilic molecules: (a) space filling structure of a phospholipid (DPPC) and (b) geometrical parameters commonly used to describe the structure of surfactants.

characterized by their static structure and dynamic, equilibrium thermal fluctuations. Because they are soft matter systems, both structure and fluctuations properties are strongly correlated (for a review, see Refs. 13 and 14). In particular, structural information on the variation in chemical composition has been obtained using neutrons[5,15–17] or electron density using x rays.[18–22] Although most of the structural and equilibrium properties of lipid membranes are now well understood, many of their dynamic features still need to be elucidated.

For the living realm, where phospholipid bilayers build the walls of cells and cellular organelles, large vesicles and small liposomes provide simple models to understand cell membrane properties: transport, fusion, or mechanical resistance.[4,10] Supported bilayers are another system that can give access to a single model membrane.

II. PHYSICS OF MEMBRANES

A. General description

The physics of fluid membranes is intrinsically a multiscale phenomenon. From a thermodynamics point of view, one can distinguish various states such as crystalline, gel, ripple, and fluid phase.[8,23] At the molecular scale, single

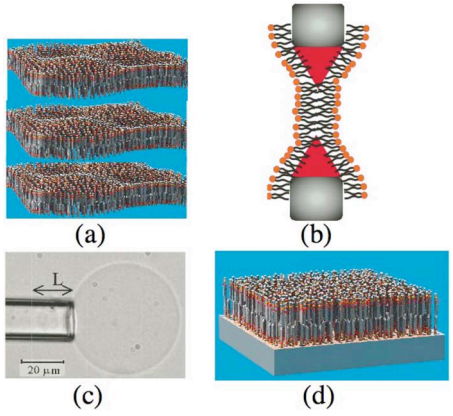

FIG. 2. Various model systems involving lipid membranes: (a) multilamellar phase; (b) black lipid membrane (BLM); (c) vesicles (which can be unilamellar or multilamellar); (d) supported lipid bilayer (SLB).

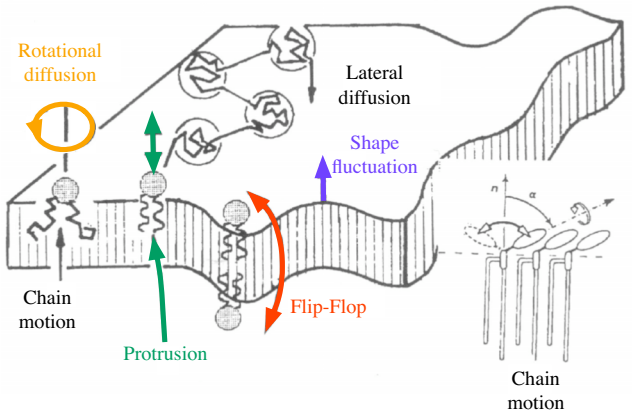

FIG. 3. Schematic representation of lipid motions in membranes (from Sackmann[23]).

phospholipids display translational, rotational, and vibrational motions (see Fig. 3),[24–26] whose relative importance is a function of the state of the assembly, and thus sensitive to external factors such as temperature, membrane tension, or hydrodynamic stresses.[23]

In turn, the collective motion of the membrane at larger length scales reveals the constitutive parameters of the membrane such as its elasticity and its internal viscosity and is also affected by the hydrodynamics of the solvent. A wide variety of physical phenomena, such as phase transitions,[27] equilibrium,[20,28] and nonequilibrium fluctuations,[29] or destabilization and topological changes[30,31] involve complex mechanisms in a range of length scales going from a nanometer to hundreds of microns. Finally, membrane-membrane or membrane-substrate interactions (often involving van der Waals, electrostatic, and hydration interactions) involve complex enthalpic and entropic contributions.

In this chapter, we give a short overview of the basic concepts of membrane statistical physics. We will first introduce the Helfrich energy at zero temperature, then discuss the influence of temperature on membrane properties. Finally, we will briefly discuss out-of-equilibrium properties.

B. Energy and stability

1. Helfrich energy at zero temperature

The theoretical study of shape and topology of fluid membranes has significantly developed since the pioneering work of Canham[11] and Helfrich.[12] To describe the bilayer physical properties at a macroscopic level, the latter introduced a phenomenological elastic energy:

$$\mathcal{H} = \frac{1}{2}\kappa \int dA(c_1 + c_2 - c_0)^2 + \bar{\kappa} \int dA c_1 c_2 + \gamma \int dA \qquad (2)$$

where dA is the differential surface element. The bilayer shape is described by the two principal curvatures c_1 and c_2 ($c_i = 1/R_i$, where R_i is the radius of curvature) (see Fig. 4). The mean curvature $H = (c_1 + c_2)/2$ and the Gaussian curvature $K = c_1 c_2$ are two invariants of the curvature tensor. The Helfrich-Canham energy can thus be seen as a Landau de-

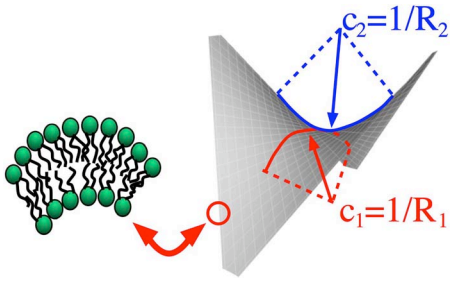

FIG. 4. Definition of the membrane principal curvatures c_i.

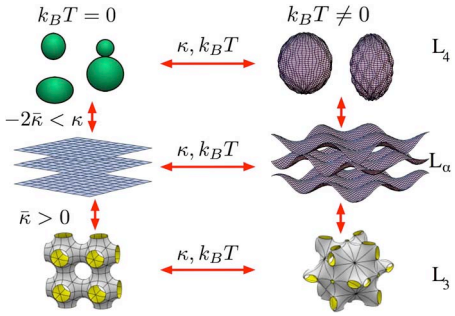

FIG. 5. Schematic phase diagram of lamellar phases. On the left, zero temperature structures. On the right, equivalent structures at nonzero temperature.

velopment in terms of curvature tensor invariants, defining some characteristic physical parameters of the bilayer. The first term is associated with the bending of the bilayer: c_0 is the spontaneous curvature of the bilayer and κ is its bending modulus. The second term is associated with the Gaussian curvature, leading to the concept of Gaussian modulus $\bar{\kappa}$. This term is related to the membrane topology via the Gauss-Bonnet theorem:

$$\iint_S c_1 c_2 dA = 4\pi(1-g), \tag{3}$$

where g is surface genus and corresponds to the number of handles ($g=0$ for a sphere and $g=1$ for a torus). This contribution to the elastic energy acts as a chemical potential controlling the number of handles in the system and is directly related to the formation of saddle points on the surface.

The third and last terms are related to the surface energy of the membrane and involve the surface tension γ.

2. Lamellar phase stability

Using this simple bending energy, it is possible to investigate the stability of a lamellar phase, i.e., a "stack of bilayers." Destabilization can occur in two ways: the formation of passages connecting bilayers or the formation of vesicles:

(1) To a first approximation, a passage is a zero-mean-curvature surface, and its energy cost is only due to the Gaussian curvature ($E_{\text{passage}} \sim -4\pi\bar{\kappa}$). The lamellar phase will form passages if $\bar{\kappa} > 0$, leading to the formation of a cubic or a sponge phase.

(2) The energy cost associated with the formation of a spherical vesicle is $E_{\text{ves}} \sim 4\pi(2\kappa + \bar{\kappa})$. Vesicles will thus form when $\bar{\kappa} < -2\kappa$.

These properties are summarized in Fig. 5.

C. Role of temperature

1. Renormalization of elastic parameters

The elastic energy introduced by Canham[11] and Helfrich[12] describes the membrane properties at zero temperature. A finite temperature T induces bilayer fluctuations. In that case, renormalization theory shows that the real membrane needs to be replaced by an effective membrane, depending on the observation length scale ξ. The projected area and the renormalized elastic parameters of the effective membrane are given by[32–35]

$$\mathcal{A}_{\text{eff}}(\xi) = \mathcal{A}_0\left[1 - \frac{k_B T}{4\pi\kappa_0}\log\left(\frac{\xi}{\delta}\right)\right], \tag{4}$$

$$\kappa_{\text{eff}}(\xi) = \kappa_0\left[1 - \frac{3k_B T}{4\pi\kappa_0}\log\left(\frac{\xi}{\delta}\right)\right], \tag{5}$$

$$\bar{\kappa}_{\text{eff}}(\xi) = \bar{\kappa}_0\left[1 - \frac{5k_B T}{6\pi\kappa_0}\log\left(\frac{\xi}{\delta}\right)\right], \tag{6}$$

where k_B is Boltzmann's constant and δ is the thickness of the bilayer. The persistence length ξ_K is defined as the characteristic length for which the bending modulus vanishes:

$$\xi_K = \delta \exp\left(\frac{4\pi\kappa_0}{3k_B T}\right). \tag{7}$$

For length scales smaller than ξ_K, the bilayer appears to be tense, whereas for larger length scales, fluctuations become important. It should be noted that ξ_K increases exponentially with $\kappa/k_B T$. With a typical value of $\delta \sim 40$ Å, we can obtain the order of magnitude of ξ_K:

(1) For $\kappa \simeq 10 k_B T$, a classical value for a membrane in the fluid phase, $\xi_K = 10^{19}$ m! This value is large compared to all characteristic length scales of the system.
(2) Values of κ of the order of $k_B T$ lead to $\xi_K \simeq 2$ μm. Large fluctuations could be observed at the micron length scale, on giant vesicles[36] or in living systems.[37]
(3) For classical microemulsions, it is usual to observe values of κ of the order of $k_B T/10$. Fluctuations are important and lead to a destabilization of the lamellar phase. The droplet size of the resulting microemulsion is fixed by ξ_K.

This simple argument leads to a phase diagram with no surfactant concentration dependence. More refined descriptions have been suggested[38] to take into account concentration effects.

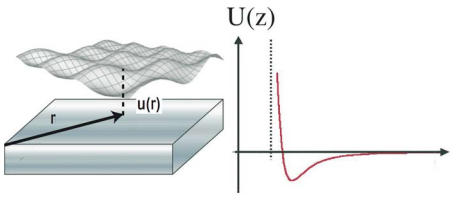

FIG. 6. Schematic picture of the thermal fluctuations of a membrane close to a substrate (at $z=0$). The membrane local position can be described by a function $u(\vec{r})$, where $\vec{r}=(x,y)$ denotes the lateral coordinates. The balance between the substrate interaction potential $U(z)$ and the entropic repulsion results in a mean interface position at $D(T,\kappa)=\overline{u(\vec{r})}$ which depends on the temperature T and the bending rigidity κ of the membrane.

2. Fluctuations around the equilibrium and Helfrich interaction

Thermal agitation induces shape fluctuations of the membrane. In the case of a planar membrane adsorbed on a solid substrate ($z=0$), the surface shape can be described in the Monge representation by the membrane position $z=u(\vec{r})=u(x,y)$ (see Fig. 6).

In these conditions, the elastic energy can be linearized as

$$\mathcal{H} \simeq \frac{1}{2}\kappa \int dxdy(\Delta u)^2 + \gamma \int dxdy(\vec{\nabla} u)^2 + \int dxdy U(u(\vec{r})). \tag{8}$$

For small fluctuations, it is possible to develop the microscopic potential $U(u(\vec{r}))$ around the equilibrium position. This leads to a quadratic energy in the membrane deformation $u(\vec{r})$; it is thus interesting to use a Fourier decomposition of $u(\vec{r})$ $(u_q(u(\vec{r},t))=1/(2\pi)^2 \int d^2\vec{q} u_q(t) e^{i\vec{q}\cdot\vec{r}})$. The different fluctuation modes are independent and the equipartition theorem can give the rms amplitude of each mode:

$$\langle |u_q|^2 \rangle = \frac{k_B T}{\tilde{U}'' + \gamma q^2 + \kappa q^4}, \tag{9}$$

where $\tilde{U}''$ is the second derivative of the effective potential.

For larger fluctuations, this approach is too naive. According to Helfrich,[12] the energy of a membrane is the sum of the external potential and the cost of bending. At finite temperature, the potential determines the fluctuation spectrum, according to the equipartition of energy. In turn, the entropic cost of fluctuations contributes to the free energy[39] and determines the average position of the membrane. If the potential depends on the position, then the effective potential felt depends on how the membrane explores the space around its equilibrium position.[40,41] The effective potential, the average position, and the fluctuation amplitude are thus coupled quantities. This entropic interaction has important experimental consequences and explains, for example, the neutral surfactant stability of lamellar phases.

We now present simple arguments first introduced by Helfrich,[39] which enable to understand this entropic interaction in the case of tensionless membranes ($\gamma=0$). Let us consider a single bilayer of bending modulus κ confined between two hard walls separated by d [Fig. 7(a)]. Each impact

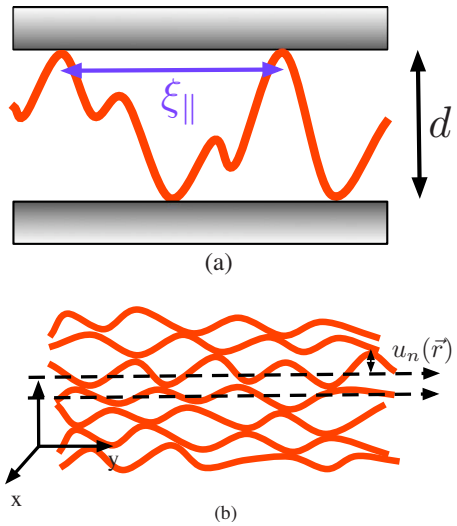

FIG. 7. Symmetrical geometries described by the Helfrich theory[39]: (a) a membrane confined between two walls; (b) a membrane confined in a multilamellar phase.

of the bilayer on the wall fully decorrelates the fluctuations, and the membrane can be seen as a collection of independent patches of size $\xi_\parallel^2$ and fluctuation amplitude d (see Fig. 7).

It is now easy to relate these two quantities using Eq. (9) (with $\tilde{U}''=0$ and $\gamma=0$):

$$\langle |u_q|^2 \rangle = \frac{k_B T}{\kappa q^4} \Rightarrow d^2 \sim \int d^2\vec{q} \langle |u_q|^2 \rangle \sim \frac{k_B T}{\kappa} \xi_\parallel^2. \tag{10}$$

The free energy per unit area $\Delta\mathcal{F}_S$ due to the bilayer confinement can then be estimated. The curvature of the surface is $1/R \sim d/\xi_\parallel^2$ and the bending energy is given by

$$\Delta\mathcal{E}_c \simeq \kappa \left(\frac{d}{\xi_\parallel^2}\right)^2. \tag{11}$$

All patches of size $\xi_\parallel^2$ are independent, and their confinement reduces their entropy by k_B,

$$-T\Delta\mathcal{S}_c \simeq \frac{k_B T}{\xi_\parallel^2}. \tag{12}$$

The final result gives the free energy of the bilayer confined between hard walls and describes the entropic interaction between the membranes and the wall. We obtain

$$\Delta\mathcal{F}_{\text{Helfrich}} \propto \mathcal{E}_c - T\Delta S \propto \frac{(k_B T)^2}{\kappa} \frac{1}{d^2}. \tag{13}$$

This is a repulsive interaction, proportional to the thermal energy $k_B T$ and inversely proportional to the bending modulus. It is usual to introduce a proportionality constant c_H to finally define the Helfrich repulsion energy as

$$V_{\text{Helfrich}} = c_H \frac{(k_B T)^2}{\kappa} \frac{1}{d^2}. \tag{14}$$

Numerous theoretical studies have been developed since the pioneering work of Helfrich.[39] Seifert[42] suggested a generalization of the Helfrich interaction in the case of membranes

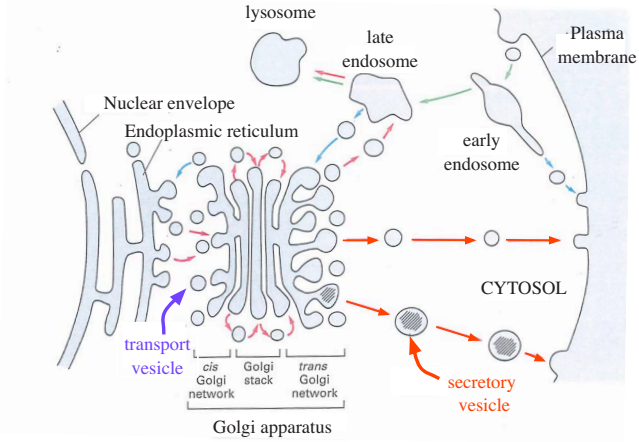

FIG. 8. Schematic representation of intracellular transport via vesicles between the endoplasmic reticulum, the Golgi apparatus, and the cell membrane (from Ref. 45).

under tension ($\gamma \neq 0$). Lipowski and Leibler[40] and Leibler and Lipowsky[41] studied the asymmetric case of a bilayer interacting with one wall in the limit of large fluctuations using group renormalization theory and introducing the concept of unbinding. A self-consistent theory was developed by Mecke *et al.*[43] to treat the asymmetric case in the small fluctuation regime for various interaction potentials.

3. Out-of-equilibrium properties

Generally, biological membranes are strongly out of equilibrium due to the presence of a large number of active biomolecules. Cell adhesion and locomotion clearly involve complex out-of-equilibrium mechanisms. Molecular transport via ion channels or pumps can also transfer momentum to the bilayer. As an example, Prost and co-workers[29,44] studied the case of an active membrane in which a nonequilibrium noise source, due to the activity of membrane proteins, is superimposed on the thermal noise. Intra- and extracellular transports through exocytosis and endocytic pathways are also complex mechanisms, which imply the formation of vesicles from the phospholipid bilayer. Such vesicles are involved in various biological processes (see Fig. 8): transport vesicles ensure transfer from the rough endoplasmic reticulum to the Golgi apparatus and secretory vesicles from the Golgi apparatus to the cell membrane, and synaptic vesicles are crucial for the transmission of information between neurons.[45]

The formation of vesicles by membrane destabilization is also an interesting problem for physicists, which involves complex physical mechanisms: nonlinear instability, complex dynamics involving viscous dissipation, and internal friction between monolayers. An important example is membrane destabilization by an electric field, which is involved in the electroformation of giant unilamellar vesicles. In a recent theoretical paper, Sens and Isambert[31] claimed that the electric field acts as a negative surface tension, which induces an undulation instability of the bilayer, and that hydrodynamic effects select the fastest-destabilized mode. These predictions are difficult to test in classical electroformation experiments, but supported double bilayers are good candidates to carry out such investigations on model systems.

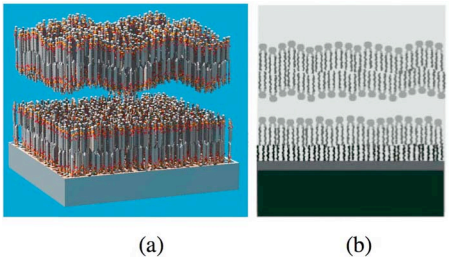

FIG. 9. (a) Supported double bilayer[5] and (b) grafted OTS-bilayer system.[49]

III. SYSTEM AND TECHNIQUES

A. System: Floating bilayers

Phospholipid bilayers deposited on a solid substrate are usually called "supported bilayers."[4] These are interesting systems that provide the opportunity to study a single bilayer with a well-defined position, allowing the use of numerous experimental techniques such as atomic force microscopy,[46] optical microscopy, fluorescence recovery after photobleaching, and x-ray or neutron scattering. These systems have been widely used to investigate various properties of phospholipid membranes.[4,23]

The investigation of the fluctuations and destabilization of a single bilayer using neutron and x-ray scatterings requires a weak interaction of the bilayer with the substrate. Several solutions have been suggested to reduce this interaction, for example, the use of a polymer cushion.[47,48] Another possibility consists in depositing two bilayers on a substrate: the first one plays the role of a spacer while the second one, usually called "floating bilayer," interacts weakly with the substrate[5] [see Fig. 9(a)]. More recently, Hughes *et al.*[49] proposed to use a mixed octadecyltrichiorosilane (OTS)-lipid spacing bilayer [see Fig. 9(b)].

These systems present many advantages. The nearly free bilayer is accessible and nonconfined, with a well-defined position. It offers the possibility to use various techniques to probe at the molecular scale the membrane dynamics on a single bilayer. Due to the relatively weak interaction of the membrane with the substrate, these systems are fragile and careful techniques are required for their preparation.

B. Characterization: Specular and off-specular reflectivities

In this section we describe briefly the scattering techniques used to investigate supported lipid bilayer properties. In a surface scattering experiment, the scattered intensity depend on the wave vector transfer $\mathbf{q}=\mathbf{k}_{sc}-\mathbf{k}_{in}$. In a specular reflectivity experiment, $\mathbf{q}$ is normal to the interface ($q_x=0$). It allows the determination of the structure and composition of thin layers in the direction perpendicular to the interface [see Fig. 10(a)]. Data analysis is complicated by loss of the phase information after the scattering event. It is therefore neces-

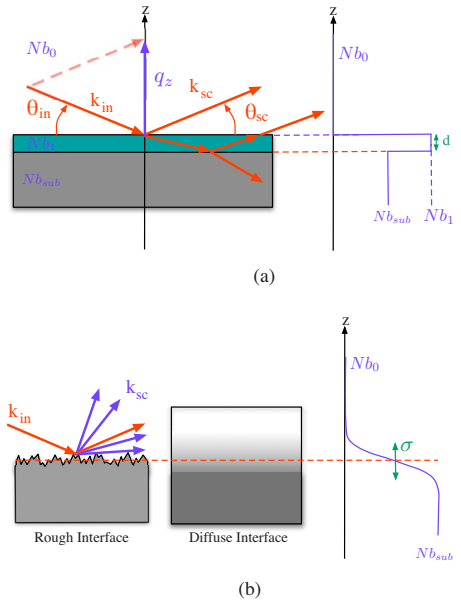

FIG. 10. (a) Specular reflectivity geometry: the signal is measured for a scattered angle θ_{sc} equal to the incident angle θ_{in}. The transfer vector $\mathbf{q}$ is normal to the sample interface, and the reflectivity data give information on the structure of the sample normal to the interface [scattering length density profile $Nb=f(z)$]. (b) In the case of a diffuse or rough interface, the scattering length density profile has a finite thickness.

sary to proceed in steps and characterize first the substrate alone, then the first adsorbed bilayer and finally the floating bilayer.[5] With this technique, the following information can be obtained on the system:

(1)the scattering length density ρ characteristic of the present atomic species;
(2)the thickness D of the layer; and
(3)the interfacial width σ between layers of different compositions usually taken into account by a Debye-Waller factor.

The physical meaning of the first two parameters is clear even though one must be careful with its interpretation. With neutron reflectivity, isotope labeling and contrast variation are highly employed to increase sensitivity.[50] Successive multicontrast characterization of the substrate, first bilayer, and double bilayer was done here (see Fig. 11).

The meaning of the third parameter is more complex. The interface between two chemically different species is never perfect on the molecular scale (see Fig. 10(b)]. Furthermore, different physical phenomena can be responsible for an apparent interface widening, for example, static *roughness* (solid substrate, vitrous polymer), dynamic fluctuations (interfacial fluctuations, lipid protrusions, polymer chains fluctuations, etc.), or the variation in the concentration of species in solution in the proximity of an interface. Finally, this parameter corresponds to an integrated mean value over all spatial length scales of the sum of all these contributions, which further complicates the analysis. Ideally, the *roughness* spectrum of the interface should be measured, that is to say, the width of each mode of the wave vector q. This is the purpose of off-specular experiments where q is not normal to the interface anymore ($q_x \neq 0$).

Off-specular synchrotron radiation measurements allowed us to get information on lateral heterogeneities and to access the lateral correlation function. Details on measurements and results may be found in Ref. 20.

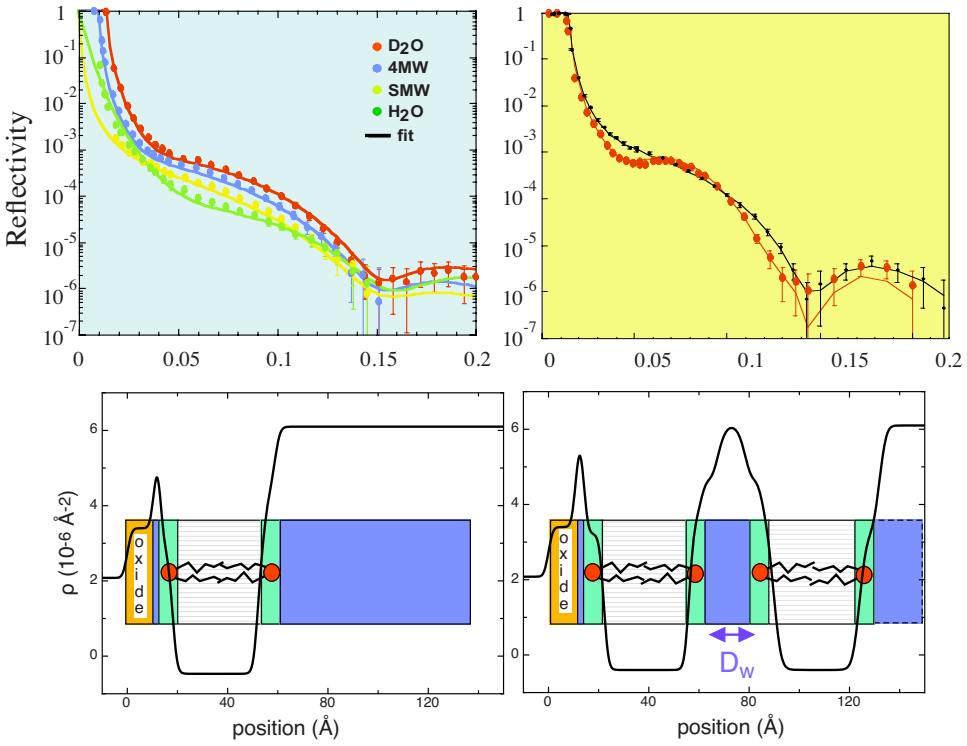

FIG. 11. (Top) Neutron specular reflectivity data (Institut Laue-Langevin, D16 and D17 instruments [75]) and (bottom) scattering length density profiles.[5,50] (Left) Single DSPC bilayer for various water contrasts; (right) double bilayer (●, red) compared to a single bilayer (+, black).

IV. STRUCTURE AND FLUCTUATIONS AT EQUILIBRIUM

A. Introduction

In this section, we will present how it is possible to access information on membrane fluctuations by neutron and x-ray scattering on supported floating bilayers. We first give some orders of magnitude. The fluctuation spectrum of a supported bilayer close to a substrate is given by Eq. (9). By integrating this expression over all the fluctuation modes (q), it is possible to express the rms fluctuation amplitude σ (note that the presence of an interaction potential suppresses the infrared divergence of the integral):

$$\sigma^2 = \langle |u|^2 \rangle = \int d^2\vec{q} \langle |u_q|^2 \rangle. \tag{15}$$

Using typical values for parameters, $U'' \simeq 10^{12}-10^{13}$ J m^{-4}, $\gamma \simeq 10^{-4}-10^{-5}$ N m^{-1}, and $\kappa \simeq 10-50$ k_BT, leads to an estimation of $\sigma < 1$ nm. This value is comparable to substrate roughness or lipid protrusions. However, near the transition, because of large density fluctuations, the bending modulus κ becomes of the order of $\sim k_BT$ and σ can reach values around 2–5 nm when going from the gel ($T < T_m$) to the fluid phase ($T > T_m$) of the lipid bilayer.

B. Indirect study of the fluctuations: Giant swelling at T_m

The transition between the gel and the fluid phase of a bilayer is called the *main transition* and the transition temperature is denoted T_m. For some phospholipids, an intermediate phase called *ripple phase*, in which the bilayer exhibits static undulations with a sawtooth shape, is observed in a narrow temperature range $T_p < T < T_m$.[27]

The gel to fluid is a highly cooperative transition where the specific heat displays a sharp maximum. A subtle thermodynamic analysis[27] allows to relate the area compressibility $\Delta\kappa_T^{\text{area}}$ to the heat capacity at constant pressure:[27]

$$\kappa_T^{\text{area}} = \frac{\gamma_{\text{area}}^2 T}{A} c_p, \tag{16}$$

where γ_{area} is a proportionality constant between the enthalpy (ΔH) and the area (ΔA) variations at the transition.[27] The compressibility $\Delta\kappa_T^{\text{area}}$ then displays a clear maximum at T_m which is the signature of large density fluctuations in the bilayer. This behavior has dramatic consequences on the membrane mechanical properties. In fact, it is possible to relate the bending modulus κ to the compressibility $\Delta\kappa_T^{\text{area}}$ by $\kappa^{-1} = 16\kappa_T^{\text{area}}/\delta^2$. Finally, it is possible to express the bending modulus as a function of thermodynamic parameters:

$$\frac{1}{\kappa} = f\frac{1}{\kappa^{\text{fluid}}} + (1-f)\frac{1}{\kappa^{\text{gel}}} + \frac{16\gamma_{\text{area}}^2 T}{\delta^2 A}\Delta c_p, \tag{17}$$

where f is the fraction of lipids in the fluid phase. This relation clearly shows that the bending modulus dramatically decreases at the melting transition. This decrease has important consequences on the floating bilayer because it implies a large increase in thermal fluctuations.

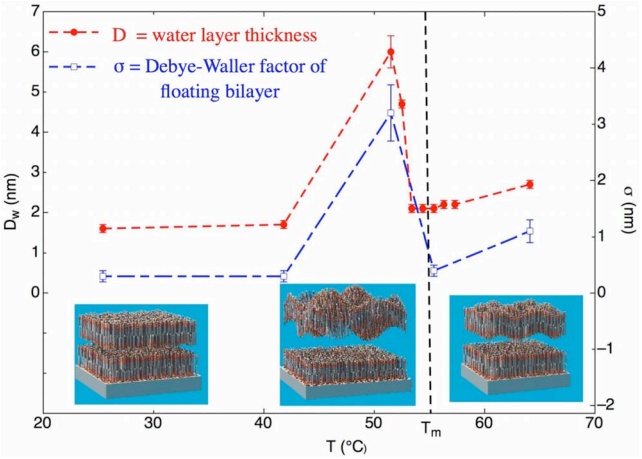

FIG. 12. Neutron reflectivity investigation of effect of temperature on a DSPC double bilayer (Ref. 76): (●, red) mean position of the floating bilayer D_w; (○, blue) rms amplitude σ of the fluctuations of the floating bilayer. The dashed line shows the melting transition temperature T_m for a multilamellar phase.

We have reported in Fig. 12 the variation in the mean distance D_w between the two bilayers and of the Debye-Waller factor σ_f associated with the floating bilayer. We observe a large increase in D_w in the vicinity of the main transition, associated with an increase in σ_f. This strong increase in the floating bilayer *roughness* could be attributed either to a static corrugation of the bilayer due to the ripple phase and to an increase in thermal fluctuations. Using specular reflectivity, it is *a priori* not possible to discriminate between these two hypotheses.

Nevertheless, we can try to interpret the floating bilayer behavior in terms of thermal fluctuations. We have developed a self-consistent model which describes the mean bilayer position and fluctuations in an asymmetrical potential[43] as a function of the dimensionless parameter $\beta = (k_BT)^2/A\kappa$ (A is the Hamacker constant). Within that framework, it is possible to deduce the value of the bending modulus from the experimental value of D_w [see Fig. 13(a)]. We can also check that the corresponding values of σ_f are in good agreement with the Debye-Waller factor determined from neutron reflectivity experiments [see Fig. 13(b)].

We observe a strong decrease of κ near the main transition temperature. The same behavior has been observed for different lipid chain lengths.[51] As shown in Fig. 13(a), the deduced values of κ are in good agreement with results obtained with macroscopic techniques on giant vesicles. This supports the validity of our interpretation in terms of thermal fluctuations.

In Sec. IV C, we will show that it is possible to go further and directly access the fluctuation spectrum of a single bilayer at the submicronic range with x-ray reflectivity.

C. Direct study of the fluctuation spectrum by x-ray scattering

In this section, we show that both specular and off-specular reflectivity measurements give direct information

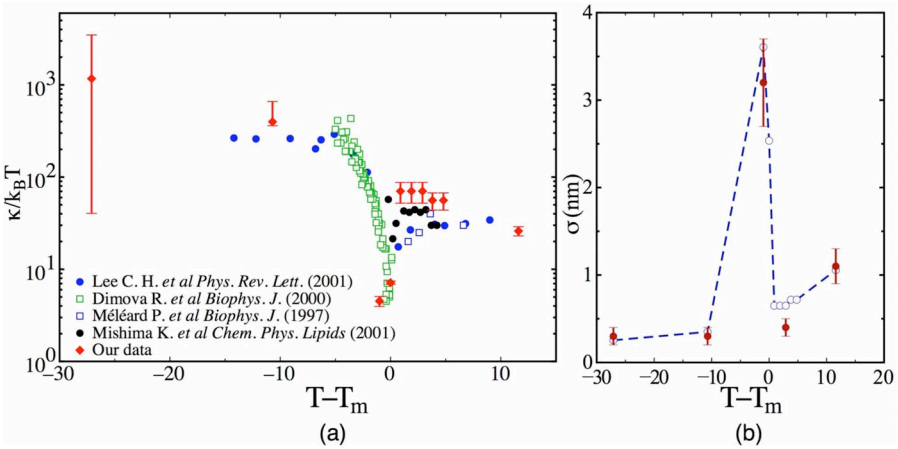

FIG. 13. (a) Variation in the bending modulus κ as a function of temperature for a DSPC bilayer: (blue, ●) from Ref. 77, (blue, □) from Ref. 64, (green, □) from Ref. 63, (black, ●) from Ref. 65, and (red, ♦) values obtained from neutron reflectivity experiments using a self-consistent theory (Ref. 43). (b) Comparison between the experimental Debye-Waller factor determined by neutron reflectivity experiments and the values from the self-consistent theory.

on the bilayer fluctuations.[20] These experiments require the use of high flux sources; all the experiments we present have been carried out at ESRF on the BM32 beamline.[52]

As shown in Sec. III B, a nonperfectly flat surface scatters x rays in off-specular directions, as well as in the specular direction due to experimental resolution. The geometry of the experiment (incident beam opening, angular resolution of detectors, etc.) must be carefully taken into account. A nice review of reflectivity techniques can be found in Ref. 53.

The off-specular signal scattered by the *rough* interface is very small. By working below the angle of total reflection ($\theta_{in} < \theta_c$), x rays penetrate only a few nanometers into the silicon substrate, minimizing diffusion by the substrate. In these conditions, the main experimental difficulty is to eliminate the diffusion by the bulk water. Figure 14 shows typical data acquisition for both a mixed OTS-distearoylphosphatidylcholine (DSPC) sample and associated background (bare silicon substrate in water). The intensity scattered by the surface is two or three orders of magnitude lower than the diffusion by bulk. The background subtraction needs to be performed carefully.

As scattering cross sections are large in the total external reflection region, a better approximation than the "kinematic" Born approximation is needed for the data analysis. Since supported bilayers only have a weak electron-density contrast with water, we can apply a perturbation theory (distorted wave Born approximation)[54] using as a reference state an ideal, flat substrate/water interface for which the scattering can be calculated exactly (Fresnel equations). We then treat the bilayer as a weak perturbation.[53] Within this approximation, the diffuse scattering cross section (intensity scattered per unit solid angle Ω in the direction $\mathbf{k}_{sc}$ per unit of incident flux in the direction $\mathbf{k}_{in}$) (see Fig. 15) is given by

$$\frac{d\sigma}{d\Omega} = \frac{d\sigma}{d\Omega}_{\text{ref}} + r_e^2 |t_{H_2O,Si}(\theta_{in})|^2 |t_{H_2O,Si}(\theta_{sc})|^2 (\hat{\mathbf{e}}_{in} \cdot \hat{\mathbf{e}}_{sc})^2 \times \left\langle \left| \int d\mathbf{r}\, \delta\rho(\mathbf{r}) e^{i\mathbf{q}.\mathbf{r}} \right|^2 \right\rangle, \quad (18)$$

where $d\sigma/d\Omega_{ref}$ corresponds to the flat substrate/water interface (r_e is the classical electron radius). Here, $t_{H_2O,Si}(\theta_{in})$ and $t_{H_2O,Si}(\theta_{sc})$ are the Fresnel transmission coefficients between water and the substrate for the grazing angle of incidence θ_{in} and the scattering angle θ_{sc}, respectively; $(\hat{\mathbf{e}}_{in} \cdot \hat{\mathbf{e}}_{sc})^2$ is a polarization factor (close to 1); the last term of Eq. (18) describes the correction ("perturbation") to $d\sigma/d\Omega_{ref}$ due to the presence of the bilayer.[20,54]

This perturbation is related to the electronic density correlation function $\langle \delta\rho(r)\delta\rho(r') \rangle$ and originates from electron-density lateral heterogeneities: this can, for instance, result from the presence of pores[55] or domains after phase separation.[56] Lateral heterogeneities can also be due to morphological perturbations: roughness,[57] static undulations (ripple phase[58,59]), protrusions,[60] thermal fluctuations,[39] etc.

In the case of height fluctuations $z(\mathbf{r}_\parallel)$, where $\mathbf{r}_\parallel = (x, y)$ is the two-dimensional, in-plane position and $\mathbf{q}_\parallel$ the reciprocal, in-plane wave vector transfer, it is possible to express the scattering cross section [Eq. (18)] in terms of a height-height correlation function:

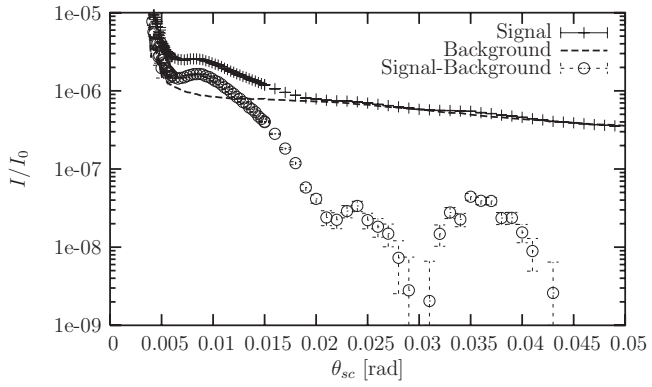

FIG. 14. Off-specular signal and background subtraction: (x) off-specular raw data (relative intensity I/I_0 vs scattering angle θ_{sc}) for a grafted OTS-floating DSPC bilayer system; dashed line: diffusion by bulk water (background); (●) signal after background subtraction, corresponding to the diffusion by the supported lipid bilayer.

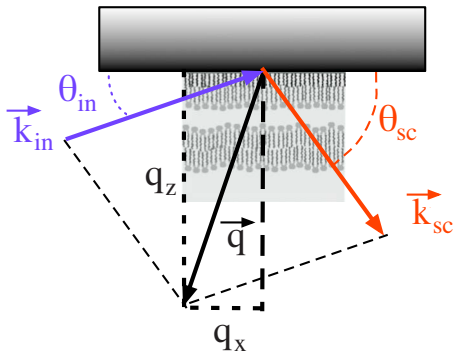

FIG. 15. X-ray off-specular reflectivity setup: the incidence angle θ_{in} is fixed just below the critical angle (~0.4°); the signal is measured for different values of the scattering angle θ_{sc}.

$$\frac{d\sigma}{d\Omega} = \frac{A}{q_z^2} r_e^2 |t_{H_2O,Si}(\theta_{in})|^2 |t_{H_2O,Si}(\theta_{sc})|^2 (\hat{\mathbf{e}}_{in} \cdot \hat{\mathbf{e}}_{sc})^2 \times \left| \int \rho(z) e^{iq_z z} dz \text{stretchy='true'} \right|^2 e^{-q_z^2 \langle z^2 \rangle} \times \int d\mathbf{r}_\parallel (e^{q_z^2 \langle z(0) z(\mathbf{r}_\parallel) \rangle} - 1) e^{i\mathbf{q}_\parallel \cdot \mathbf{r}_\parallel}. \quad (19)$$

The scattering intensity is then directly related to the bilayer fluctuation spectrum:

$$\langle u_{q_\parallel} u_{-q_\parallel} \rangle = \frac{k_B T}{U'' + \gamma q_\parallel^2 + \kappa q_\parallel^4} \quad (20)$$

and also gives access to bilayer-substrate correlations. Figure 16 shows the comparison between experimental off-specular data and the calculated scattering function. The blue curve describes the diffusion due to the silicon substrate roughness, as described by Palasantzas.[57] The dashed black curve corresponds to the diffusion by a fluctuating bilayer and the red one takes into account all contributions: bilayer roughness, membrane fluctuations, and bilayer-substrate correlation. By fitting the curve, we can extract the values of the bending modulus, the surface tension, and the second derivative of the potential in the gel and fluid phases.[20]

V. SINGLE BILAYER DESTABILIZATION

A. Destabilization at the main transition: Vesicle formation

Lipid bilayer properties undergo several changes at the main transition. The area per lipid increases by about 25% and the bending modulus strongly decreases due to large density fluctuations.[27,61] We have shown previously that these dramatic decreases in the bending modulus can account for the large swelling observed for a double bilayer at the main transition. It is interesting to investigate whether it is possible to go further and induce a complete unbinding of the floating bilayer.

We have recently reported results showing that this swelling can indeed turn into a complete destabilization.[62] Upon heating zwitterionic lipid bilayers deposited on glass slides,

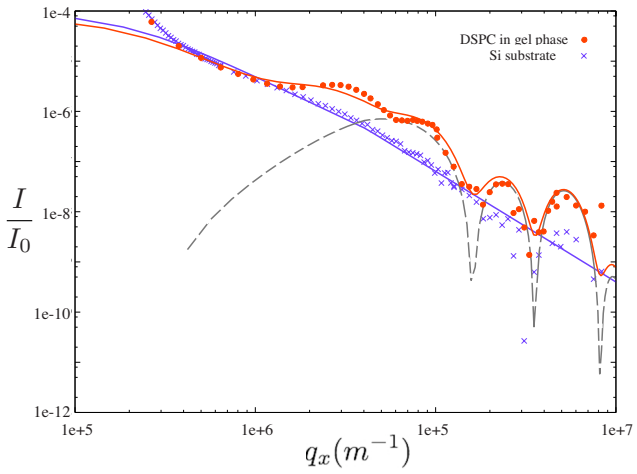

FIG. 16. Off-specular reflectivity curves: (x) silicon substrate; (+) floating DSPC bilayer in the gel phase. The blue curve corresponds to a fit of the data with a roughness spectrum for the substrate as in Ref. 57, the black line corresponds to a fit of the data for a single bilayer fluctuating with a spectrum as Eq. (15), and the red line takes into account the bilayer-substrate correlations.

unbinding was observed at the main gel-to-fluid transition of the lipids, and led to the formation of micrometric vesicles of well-defined size (see Fig. 17). This phenomenon occurred with double as well as single supported bilayers; in the latter case, the typical size of the vesicles formed was significantly smaller.

Bilayer destabilization can be induced by either mechanical buckling to release excess area and/or thermal unbinding due to increased amplitude of fluctuations.[40,41] However, neither vesicle formation nor large length scale defects have been observed on silicon substrates by microscopy or neutron reflectivity, which indicates that supported bilayers can release excess area without dramatic structural modifications. Self-consistent analysis of neutron reflectivity,[43] macroscopic measurements of κ on vesicles,[63–65] and predictions deduced from heat capacity measurements[56] indicate that κ decreases from $\sim 200 k_B T$ in the gel phase to $1-3 k_B T$ at the transition. Membrane unbinding,[40,41,43] bilayer position, and fluctuations are controlled by the dimensionless parameter β. Unbinding occurs for $\beta_u \sim 0.33$. With experimental values for κ, we find that a decrease in the adhesion energy by a factor of 2 could be enough to induce unbinding at the transition, which is consistent with recent models for rough substrates.[66]

In any case, vesicle formation requires large bending of the bilayer. The persistence length of the membrane ξ_K defined in Eq. (7) gives the length scale beyond which the renormalized bending modulus is smaller than $k_B T$.[33] One finds that a value of κ around $1.8 k_B T$ is required to have $\xi_K \sim 5$ μm; assuming that the vesicle size is correlated with ξ_K, this is very consistent with our experimental results. However, the actual mechanism is probably more complex and parameters such as the hydrodynamics of the solvent should also be considered.[31]

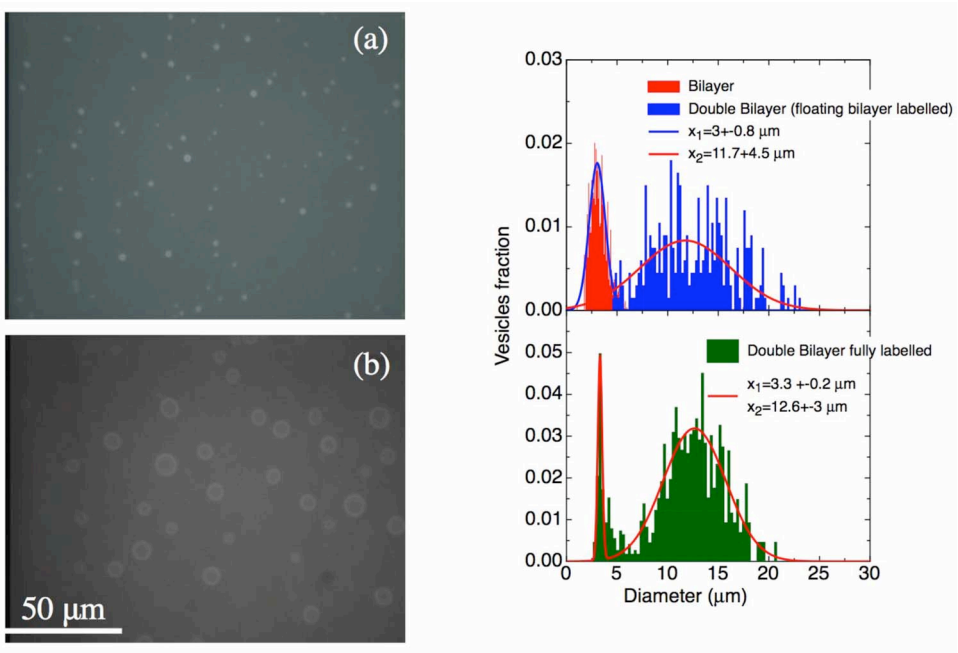

FIG. 17. Vesicle formation at the main transition for (a) a single DPPC bilayer on a glass substrate; (b) a double DPPC bilayer on a glass substrate [fluorescence microscopy images; bilayers contain 1% NBD (7-nitro-2-1,3-benzoxadiazol-4-yl)-labeled lipids]. On the right, vesicle size distributions obtained with varying selective fluorescent labeling of the samples (one leaflet only or all leaflets).

B. Destabilization by an electric field

The strong influence of electric fields on lipid bilayers is interesting both from a fundamental point of view and for practical aspects, and has consequently received an important research effort. Large electric fields can lead to the formation of long-lived pores in the bilayer[67,68] and are also used to introduce macromolecules in vesicles or cells by endocytosis.[69] Smaller alternative electric fields are commonly used to destabilize lipid bilayers in order to form giant unilamellar vesicles[70,71] in the so-called electroformation technique. Because they are almost free of defects, double bilayer systems are promising candidates to reach a better understanding of the mechanism of vesicle formation in a well-defined geometry.

Although it is a widely used technique, the mechanism involved in vesicle electroformation is not well understood yet. A recent theoretical paper[31] suggested that the electric field E acts as a "negative surface tension" $-\Gamma_{el}$ (with $\Gamma_{el} > 0$), given by

$$-\Gamma_{el} = -\epsilon_m \left(\frac{\chi_m}{\chi_s}\right)^2 E^2 \delta < 0, \tag{21}$$

where χ_m (χ_s) are the membrane (solvent) conductivities, and ϵ_m and δ are the membrane permittivity and thickness.

Let us include this negative surface tension in the fluctuation spectrum [Eq. (20)]:

$$\langle u_q u_{-q} \rangle = \frac{k_B T}{U'' + (\gamma - \Gamma_{el}) q^2 + \kappa q^4}. \tag{22}$$

This clearly shows that all long wavelength modes $q < q_{stat} = \sqrt{\Gamma_e / \kappa}$ are unstable and that an electric field induces an undulation instability of the bilayer. Sens and Isambert[31] also showed that hydrodynamic effects select the fastest-destabilized mode.

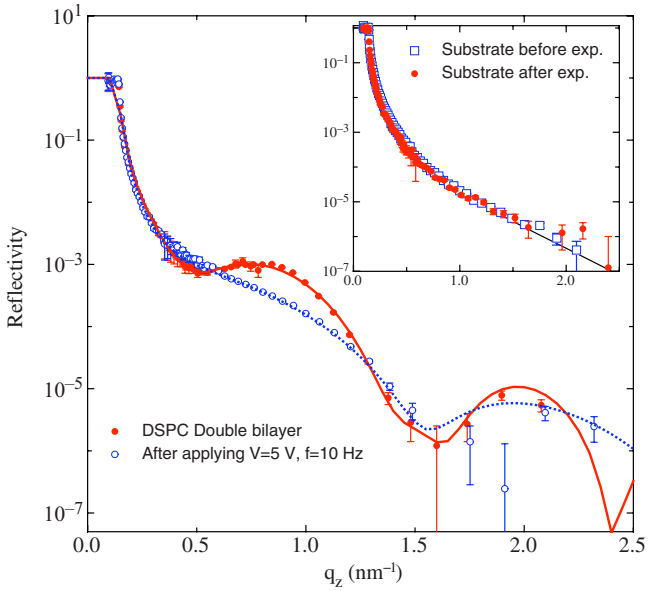

FIG. 18. Reflectivity curves: (●) double DSPC bilayer in 0.35 mM $CaCl_2$ and best fit with a double bilayer model (full line); (○) after applying a (10 V, 10 Hz) field and best fit with a single bilayer model (dashed line). In the inset, reflectivity curves for the bare substrate before and after the experiment (and best fit with a silicon oxide layer model). The sample cell consists of two 5×5 cm^2 silicon wafers separated by a 1 mm thick insulating spacer; one of the wafers holds the DSPC double bilayer. Data collected on the reflectometer D17[75] at the ILL.

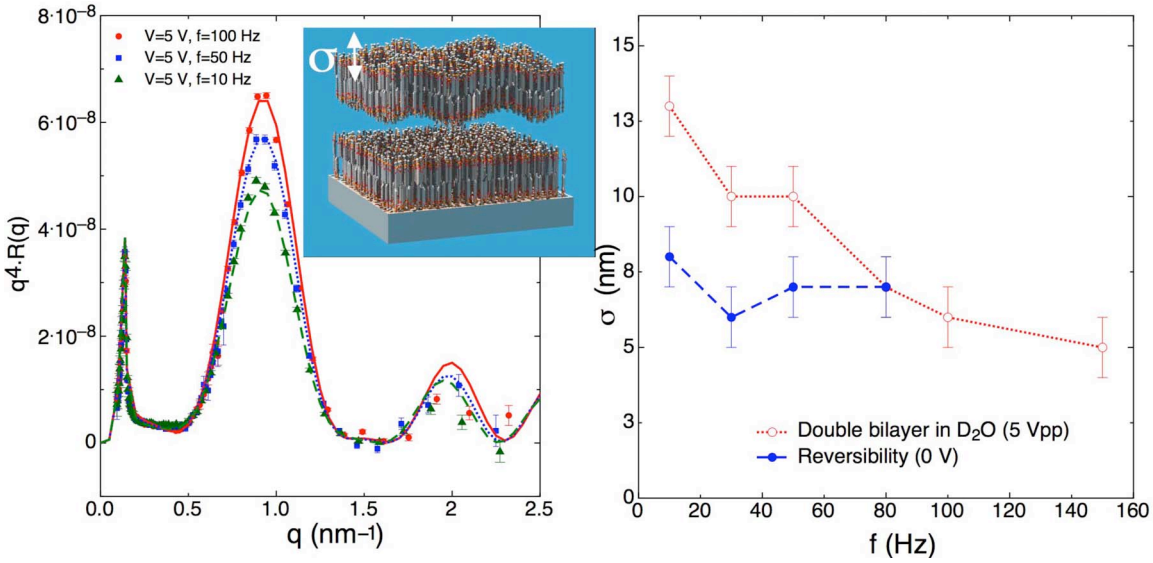

FIG. 19. Effect of the electric field frequency on the floating bilayer roughness. A $V_{pp}=5$ V ac field is applied to a DSPC double bilayer in D_2O (distance between electrodes is 1 mm). (Left) Modification of the reflectivity curve with decreasing frequency of the electric field; the lines are best fits obtained with a nine-slab model, varying essentially the roughness of the floating bilayer. (Right) Corresponding bilayer roughness σ vs electric field frequency f; values deduced from best fits of the reflectivity curves. (●) double bilayer under electric field; (○) reversibility test for each frequency (no electric field).

These predictions are difficult to test in classical electroformation experiments. As a matter of fact, the initial system is usually a rather disordered lamellar phase, obtained by hydration of a dry lipid film and, consequently, the result is very polydisperse in both size and degree of lamellar order. Recently, Constantin *et al.*[72] reported the first study of membrane destabilization by an electric field on a more controlled system: a solid-supported fully hydrated oriented lamellar phase (from 10 to 3000 bilayers). They observed, for the first time, individual peeling of the bilayers but were not able to confirm or refute the existence of an electrodynamic instability.

We reported recently the first study of the destabilization by an electric field of a unique membrane: the floating bilayer of a double bilayer system.[73] The main result of this work was the observation of the complete unbinding of the floating bilayer, by application of an electric field on a double DSPC bilayer in a $CaCl_2$ solution. The effect occurs at low frequency (10 Hz) and for a voltage amplitude higher than 5 V. Figure 18 shows reflectivity data before and after applying the electric field. The curves correspond to the best fits obtained with a nine-slab model and are consistent with previous multicontrast neutron reflectivity experiments.[5] After the unbinding, we still observed the presence of the first bilayer, without any major change in structure, but slightly shifted away from the substrate. After removing the bilayer by cleaning the substrate, we could check that the silicon oxide layer was unmodified, and therefore that there was no significant formation of porous silicon oxide (Fig. 18 inset).

This complete unbinding of the floating bilayer was very sudden. However, in a lower-conductivity electrolyte, we were able to observe previous steps of the destabilization. The progressive modification in the reflectivity curves is reported in Fig. 19.

At high frequencies ($f>100$ Hz), changes appeared to be irreversible and involved mainly the first bilayer. They could originate from the formation of pores or larger holes due to hydrodynamic stress. At the same time, the second bilayer structure was unmodified.

At lower frequencies, modifications mainly involved the floating bilayer roughness and were reversible. It thus

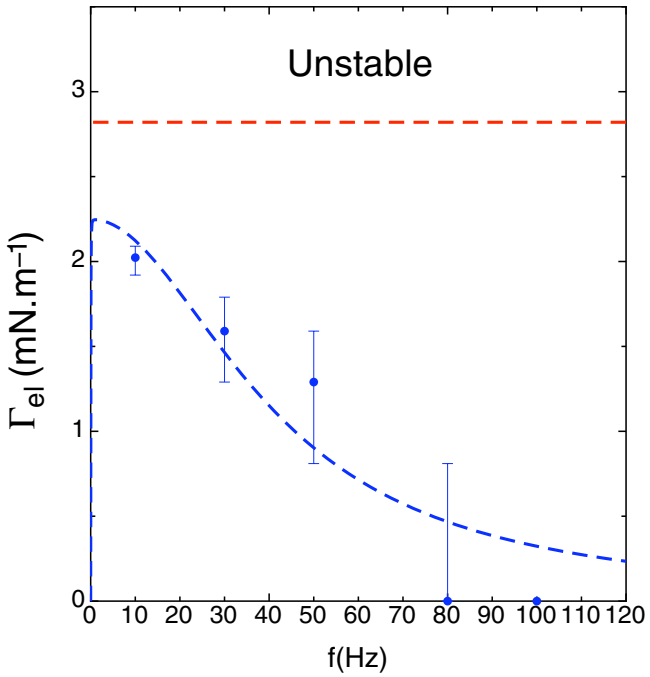

FIG. 20. Electric "negative surface tension" Γ_{el} as a function of frequency [values derived from experimental data using Eq. (22)]. The dark region on the left corresponds to the frequency limit ($f\sim5$ Hz) below which silicon oxidation was observed.

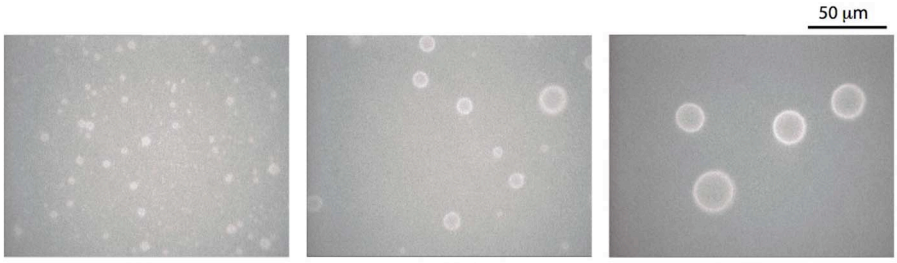

FIG. 21. Vesicles are formed by application of a low-frequency electric field ($f \sim 5$ Hz) to a single supported DPPC bilayer on glass (fluorescence microscopy images; bilayers contain 1% NBD-labeled lipids). The sample cell consists of two ITO-coated glass slides separated by a 2 mm insulating spacer. Successive images show the vesicles located immediately above the substrate after different durations of the field; the average size of the vesicles progressively increases, while their surface density decreases, as they likely detach from the surface.

seemed physically reasonable to fit the double bilayer reflectivity curves under electric field by varying essentially the bilayer roughness and the water layer thickness; average percentages of solvent within the bilayers were also allowed to vary, accounting for the induced formation of defects or pores in the membranes.

The irreversible destabilization of the floating bilayer thus seems to be preceded by a reversible increase in its roughness, as reported on Fig. 19. It is possible to describe this roughness in terms of thermal fluctuations. Previous x-ray off-specular experiments[20] showed on very similar samples (a fluid DSPC bilayer deposited on a hybrid OTS-DSPC bilayer) that $\kappa \simeq 40\ k_B T$ and $\gamma \simeq 0.5$ m N m^{-1}. Using these experimental results, we can determine the value of U'' corresponding to the correct experimental value of σ measured without any electric field. Following this method, we obtain $U'' \simeq 10^{13}$ J m^{-4}. This value is in good agreement with theoretical estimations using a van der Waals potential.[9]

Using the experimental determinations of σ, γ, κ, and U'', we can now evaluate the electric surface tension Γ_{el} using Eq. (22). The results are reported in Fig. 20 and show that field frequency is an important parameter in membrane destabilization. We do not observe any modification in the bilayer above 100 Hz, whereas the effect becomes important below 10 Hz, in good agreement with previous observations by Constantin *et al.*[72]

Using fluorescence optical microscopy, we recently showed that it was also possible to destabilize a single bilayer supported on glass with a perpendicular low-frequency electric field. In that case, we have been able to observe that the destabilization leads to the formation of vesicles, the average size of which progressively increased with time, reaching about 10 μm after 1.5 h.[74] The results are summarized in Fig. 21.

VI. CONCLUSION

In this article, we have shown how neutron and x-ray scattering can be used to obtain information on the physics of lipid membranes and, in particular, on their fluctuations and destabilization. We have used single and double supported bilayers deposited on flat substrates, which are well-controlled systems, and give access to an ideal, well-localized lipid membrane. Specular reflectivity (of neutrons or x rays) provides average structural information on the samples: the thickness and composition of each layer and rms roughness. The study of the off-specular scattering of x rays gives access to lateral inhomogeneities of the interface, hence, to the fluctuation spectrum of the membrane. A thorough analysis of experimental data allowed us to determine the surface tension and the bending modulus of a floating bilayer. However, it is important to note that this analysis requires a very careful subtraction of the background signal and close-to-perfect samples.

We then focused on the phenomenon of membrane destabilization. Unbinding of supported bilayers can occur at the main gel-to-fluid transition, following from the strong decrease in the bending rigidity and the associated softening of the bilayer. Destabilization can also result from the application of a low-frequency ac electric field in the fluid phase. In both cases, neutron reflectivity gives access to the first steps of the destabilization since it allows to detect small modifications of the system at the nanometer length scale. When the membrane eventually unbinds, complementary experimental techniques become useful to observe the vesicles that can form as a result of this process. We have used fluorescence microscopy to observe vesicle formation from a single supported bilayer, either at the transition or under electric field. These vesicles tend to have a well-defined size, which is likely to depend on intrinsic parameters of the sample (substrate and lipid nature, distance to the substrate, etc.) or the environment (temperature, field amplitude or frequency, etc.). These results highlight the strong potential of supported bilayers as model systems to study the process of bilayer destabilization and the parameters at stake in the selection of vesicle size. This should ultimately give better understanding of this process, which is of crucial importance in many biological phenomena, as well as a valuable tool for biophysicists.

ACKNOWLEDGMENTS

The authors wish to thank Jean Daillant, Linda Malaquin, Edith Bellet-Amalric, Alan Braslau, and François Graner for their participation to the experiments and for illuminating discussions.

[1]L. Auvray, J. Charvolin, and J. Di Micoli (unpublished).
[2]G. Porte, Cours sur les Sytèmes Moléculaires Organisés, Ecole d'été, Les Houches, 1996 (unpublished).
[3]J. Seddon and R. Templer, *Structure and Dynamics of Membranes: From Cells to Vesicles* (Springer, New York, 1995), Vol. 1A.
[4]E. Sackmann, Science **271**, 43 (1996).
[5]T. Charitat, E. Bellet-Amalric, G. Fragneto, and F. Graner, Eur. Phys. J. B **8**, 583 (1999).
[6]T. H. Watts, A. A. Brian, J. W. Kappler, P. Marrack, and H. M. McConnell, Proc. Natl. Acad. Sci. U.S.A. **81**, 7564 (1984).
[7]R. Richter and A. Brisson, Biophys. J. **88**, 3422 (2005).
[8]J. Katsaras and T. Gutberlet, *Lipid Bilayers*, Biological Physics Series (Springer, New York, 2000).
[9]R. Lipowsky, *Handbook of Biological Physics* (Elsevier, New York, 1995), Vol. 1.
[10]O. Mouritsen and O. Andersen, *In Search of a New Biomembrane Model, Biologiske Skrifter* (The Royal Danish Academy of Science and Letters, Copenhagen, 1998).
[11]P. Canham, J. Theor. Biol. **26**, 61 (1970).
[12]W. Helfrich, Z. Naturforsch. C **28**, 693 (1973).
[13]J. Nagle and S. Tristram-Nagle, Biochim. Biophys. Acta **1469**, 159 (2000).
[14]J. F. Nagle and S. Tristram-Nagle, Curr. Opin. Struct. Biol. **10**, 474 (2000).
[15]D. Constantin, U. Mennicke, C. Li, and T. Salditt, Eur. Phys. J. E **12**, 283 (2003).
[16]T. Salditt, C. Münster, C. Mennicke, U. Ollinger, and G. Fragneto, Langmuir **19**, 7703 (2003).
[17]J. Lemmich, K. Mortensen, J. H. Ipsen, T. Hönger, R. Bauer, and O. Mouritsen, Phys. Rev. E **53**, 5169 (1996).
[18]J. Nagle, R. Zhang, S. Tristam-Nagle, W. Sun, H. Petrache, and R. Suter, Biophys. J. **70**, 1419 (1996).
[19]T. Salditt, C. Li, A. Spaar, and U. Mennicke, Eur. Phys. J. E **7**, 105 (2002).
[20]J. Daillant, E. Bellet-Amalric, A. Braslau, T. Charitat, G. Fragneto, F. Graner, S. Mora, F. Rieutord, and B. Stidder, Proc. Natl. Acad. Sci. U.S.A. **102**, 11639 (2005).
[21]C. E. Miller, J. Majewski, T. Gog, and T. L. Kuhl, Phys. Rev. Lett. **94**, 238104 (2005).
[22]C. E. Miller, J. Majewski, E. B. Watkins, D. J. Mulder, T. Gog, and T. L. Kuhl, Phys. Rev. Lett. **100**, 058103 (2008).
[23]E. Sackmann, *Handbook of Biological Physics* (Elsevier Science, New York, 1995), pp. 213–303.
[24]M. C. Rheinstädter, C. Ollinger, G. Fragneto, and T. Salditt, Phys. Rev. Lett. **93**, 108107 (2004).
[25]M. C. Rheinstädter, T. Seydel, and F. Demmel, Phys. Rev. E **71**, 061908 (2005).
[26]J. S. Hub, S. T. M. C. Rheinstädter, and B. L. de Groot, Biophys. J. **93**, 3156 (2007).
[27]T. Heimburg, Biochim. Biophys. Acta **1415**, 147 (1998).
[28]J. Pécréaux, H.-G. Döbereiner, J. Prost, J. F. Joanny, and P. Bassereau, Eur. Phys. J. E **13**, 277 (2004).
[29]J. B. Manneville, P. Bassereau, S. Ramaswamy, and J. Prost, Phys. Rev. E **64**, 021908 (2001).
[30]X. Michalet, D. Bensimon, and B. Fourcade, Phys. Rev. Lett. **72**, 168 (1994).
[31]P. Sens and H. Isambert, Phys. Rev. Lett. **88**, 128102 (2002).
[32]W. Helfrich, Z. Naturforsch. **28c**, 510 (1974).
[33]L. Peliti and S. Leibler, Phys. Rev. Lett. **54**, 1690 (1985).
[34]F. David and S. Leibler, J. Phys. II **1**, 959 (1991).
[35]D. Sornette and N. Ostrowsky, *Micelles, Membranes, Microemulsions, and Monolayers* (Springer, New York, 1994).
[36]X. Michalet, Ph.D. thesis, Université Paris VII, 1994.
[37]F. Brochard and J.-F. Lennon, J. Phys. (Paris) **36**, 1035 (1975).
[38]D. Morse, Phys. Rev. E **50**, 2423 (1994).
[39]W. Helfrich, Z. Naturforsch., A: Phys. Sci. **33**, 305 (1978).
[40]R. Lipowsky and S. Leibler, Phys. Rev. Lett. **56**, 2541 (1986).
[41]S. Leibler and R. Lipowsky, Phys. Rev. B **35**, 7004 (1987).
[42]U. Seifert, Phys. Rev. Lett. **74**, 5060 (1995).
[43]K. R. Mecke, T. Charitat, and F. Graner, Langmuir **19**, 2080 (2003).
[44]J. Prost, J.-B. Manneville, and R. Bruinsma, Eur. Phys. J. B **1**, 465 (1998).
[45]B. Alberts, A. Johnson, J. Lewis, M. Raff, K. Roberts, and P. Walter, *Molecular Biology of the Cell* (Garland Science, New York, 2007).
[46]C. Leidy, T. Kaasgaard, J. H. Crowe, O. Mouritsen, and K. Jørgensen, Biophys. J. **83**, 2625 (2002).
[47]M. Wagner and L. Tamm, Biophys. J. **79**, 1400 (2000).
[48]E. Sinner and W. Knoll, Curr. Opin. Chem. Biol. **5**, 705 (2001).
[49]A. V. Hughes, A. Goldar, M. C. Gestenberg, S. J. Roser, and J. Bradshaw, Phys. Chem. Chem. Phys. **4**, 2371 (2002).
[50]G. Fragneto, E. Bellet-Amalric, T. Charitat, P. Dubos, F. Graner, and L. Perino-Galice, Physica B (Amsterdam) **276-278**, 501 (2000).
[51]G. Fragneto, T. Charitat, E. Bellet-Amalric, R. Cubitt, and F. Graner, Langmuir **19**, 7695 (2003).
[52]European Synchotron Research Facilities, beam line BM 32, http://www.esrf.fr/exp_facilities/BM32/index.htm
[53]J. Daillant and M. Alba, Rep. Prog. Phys. **63**, 1725 (2000).
[54]J. Daillant and A. Sentenac, in *X-ray and Neutron Reflectivity: Principles and Applications*, Lecture Notes in Physics Vol. m58, edited by J. Daillant and A. Gibaud (Springer-Verlag, Heidelberg, 1999), pp. 121–162.
[55]P. Bassereau and F. Pincet, Langmuir **13**, 7003 (1997).
[56]T. Heimburg, *Planar Lipid Bilayers (BLMs) and Their Applications* (Elsevier, Amsterdam, 2003), pp. 269–293.
[57]G. Palasantzas, Phys. Rev. B **48**, 14472 (1993).
[58]R. P. Rand, D. Chapman, and K. Larsson, Biophys. J. **15**, 1117 (1975).
[59]T. Heimburg, Biophys. J. **78**, 1154 (2000).
[60]J. N. Israelachvili and H. Wennerstrom, J. Phys. Chem. **96**, 520 (1992).
[61]T. Heimburg, *Planar Lipid Bilayers (BLMs) and Their Applications* (Elsevier, Amsterdam, 2003), pp. 269–293.
[62]S. Lecuyer and T. Charitat, Europhys. Lett. **75**, 652 (2006).
[63]R. Dimova, B. Pouligny, and C. Dietrich, Biophys. J. **79**, 340 (2000).
[64]P. Méléard, C. Gerbaud, T. Pott, L. Fernandes-Puente, I. Bivas, M. Mitov, J. Dufourcq, and P. Bothorel, Biophys. J. **72**, 2616 (1997).
[65]K. Mishima, S. Nakamae, H. Ohshima, and T. Kondo, Chem. Phys. Lipids **110**, 27 (2001).
[66]P. S. Swain and D. Andelman, Langmuir **15**, 8902 (1999).
[67]J. C. Weaver and Y. A. Chizmadzhev, Bioelectrochem. Bioenerg. **41**, 135 (1996).
[68]H. Isambert, Phys. Rev. Lett. **80**, 3404 (1998)
[69]Y. Rosemberg and R. Korenstein, Bioelectrochem. Bioenerg. **42**, 275 (1997).
[70]M. I. Angelova and D. Dimitrov, Faraday Discuss. Chem. Soc. **81**, 303 (1986).
[71]M. I. Angelova, S. Soleau, P. Méléard, J.-F. Faucon, and P. Bothorel, Prog. Colloid Polym. Sci. **89**, 127 (1992).
[72]D. Constantin, C. Ollinger, M. Vogel, and T. Salditt, Eur. Phys. J. E **18**, 273 (2005).
[73]S. Lecuyer, G. Fragneto, and T. Charitat, Eur. Phys. J. E **21**, 153 (2006).
[74]S. Lecuyer and T. Charitat (unpublished).
[75]R. Cubitt and G. Fragneto, Appl. Phys. A **A74**, S329 (2002).
[76]G. Fragneto, T. Charitat, F. Graner, K. Mecke, L. Perino-Gallice, and E. Bellet-Amalric, Europhys. Lett. **53**, 100 (2001).
[77]C.-H. Lee, W.-C. Lin, and J. Wang, Phys. Rev. E **64**, 020901 (2001).